THE ASTRONOMICAL JOURNAL VOLUME 110, NUMBER 3 SEPTEMBER 1995

INFRARED LIGHT CURVES AND ABSOLUTE PARAMETERS OF THE ACTIVE BINARY RT ANDROMEDAE

M. J. ARÉVALO AND C. LÁZARO
Departamento de Astrofísica, Universidad de La Laguna, 38206 La Laguna, Tenerife, Spain; and Instituto de Astrofísica de Canarias, 38200 La Laguna, Tenerife, Spain
Electronic mail: mam@ll.iac.es, clh@ll.iac.es

A. CLARET
Instituto de Astrofísica de Canarias, 38200 La Laguna, Tenerife, Spain
Electronic mail: claret@iaa.es

Received 1995 May 18; revised 1995 May 30

ABSTRACT

We present the first light curves in the infrared J and K filters, obtained in different runs during 1990, 1991, and 1994. The solutions of these IR light curves together with the previous determinations, gathered from visual light curves and spectroscopic studies, finally yield stellar parameters that can be accepted with confidence. The study of the $(V-\lambda)$ observed colors, by comparison with tabulated colors of normal stars, indicates that they correspond to those expected if RT And components have G0 V and K2 V spectral types. The comparison with ATLAS stellar atmosphere models gives effective temperatures about 6000 and 4900 K, for the primary and secondary star, respectively. From the visual-infrared photometry there is no evidence of an IR excess in the system, and its distance is determined to be 103 pc. We have compared the absolute stellar parameters derived from the light curve solutions with new evolutionary models for solar composition, and discussed the age and evolutionary state of this binary system. While the mass and radius of the primary star locates it close to the main sequence, with an age of about 1.4×10^9 yr, the secondary star seems to be oversized for its mass, and some sort of interacting episode in the evolutionary history of this detached binary is not discarded. © *1995 American Astronomical Society.*

1. INTRODUCTION

Astronomers have been looking at RT And (BD +52°3383A) since the beginning of this century (Deichmueller 1901; Zinner 1916; Gadomski 1928), but its first photometric light curves were not obtained until the late forties by Gordon (1948, 1955). After those observations, this variable binary, currently considered to be a member of the short-period RS CVn class (Hall 1976), has been the subject of extensive photometric observation programmes by a number of different authors (Kristenson 1967; Dean 1974; Dumitrescu 1973, 1974; Dapergolas *et al.* 1988, 1991, 1992, 1994; Mancuso *et al.* 1979a, 1979b, 1979c, 1981; Milano *et al.* 1981, 1986; Zeilik *et al.* 1982, 1988a, 1989a; Gordon *et al.* 1990, among others).

The photometric light curves of RT And in the visual range reveal interesting features. From one observation to another, irregularities or fluctuations in the brightness at both quadratures and also in the depth of its eclipses are seen. These photometric variations have been interpreted as being produced by large cool starspots over the surface of the primary star. Zeilik *et al.* (1989b) reanalyzed an extensive data set of published visual light curves together with their own. They attempted to define clean geometric parameters after subtraction of the maculation waves, inferring also the physical parameters of the cool starspots. An interesting result they report is that one large starspot can account for the photometric maculation effects displayed by the star since 1920. The stellar longitude of these active regions, like in other RS CVn short-period systems such as SV Cam (Zeilik *et al.* 1988b), tends to fall within precise active belts located near 90° and 270°. It is especially interesting to note the variability (more enhanced at shorter wavelengths) shown at the beginning and the end of both eclipses; this occurs over a short time scale, and its characteristics are difficult to explain within the activity picture in terms of starspots or flares. A considerable dip in the light curves around orbital phase 0.3 has been observed sometimes (Milano *et al.* 1986).

Via spectroscopy, Payne-Gaposchkin (1946) obtained the first radial velocity curves of both components and determined their spectral types to be G0 V and K0 V. Analyzing the same spectra, Kron (1950) detected weak emission in the Ca II H and K lines, with variable intensity along the orbital period. Low-resolution spectroscopy was carried out by Mancuso *et al.* (1981), who find the spectral types of the components to be F8−G0 V and K0−2 V. Recently, RT And was included in two different spectroscopic observing programmes (Popper 1994; Wang & Lu 1993). The new radial velocity curves, in combination with the light curves results, produce better physical parameters for the system. A study of the Hα, Hβ, and Ca II infrared triplet lines, using echelle spectroscopy with orbital phase resolution, has recently been conducted by the present authors (Lázaro & Arévalo 1994; Arévalo & Lázaro 1995).

RT And has been observed in other spectral ranges, such as the UV by means of the *IUE* satellite (Budding *et al.* 1982). Like the other such binaries of the short-period RS CVn group, RT And presents emission in the Mg H and K lines, indicating a high degree of chromospheric activity. RT And was not detected as a radio source (6 cm) in the survey of Drake *et al.* (1986). As far as we know, this binary system has not been included as a target in any x-ray observing run, and no previous observations in the infrared (IR) range have been reported.

We have carried out an infrared monitoring programme of RS CVn systems, devoting special attention to the short-period group (see Arévalo & Lázaro 1994). If the observed irregularities in the light curves of these systems are due to the obscuration effects of starspots, we can expect the contribution at longer wavelengths to be lower (in fact no corrections for distortion waves are needed in most of the observed stars). Furthermore, the secondary eclipse is better defined in the IR, due to the different spectral types of the stellar components in some of these binaries. In this way, the parameters resulting from the light curves observed in the IR range could improve previous solutions inferred from visible photometry. Photometric solutions of these eclipsing binaries, together with the new orbital parameters obtained by Popper (1993, 1994), may provide more accurate values for the masses and radii of their components, which is highly needed to allow reliable evolutionary studies. On the other hand, the possible existence of an IR excess, as a characteristic property of this group of active stars, is still an open question which calls for further observations. In the next sections we present the results obtained from our IR observations of RT And.

2. THE OBSERVATIONS

The infrared observations presented in this work were collected during different runs. The first was in 1990 August (from 9th to 17th), and allowed us to obtain the first complete IR light curves in the J and K filters. New observations were later conducted in 1991 January, 1992 August, and 1994 January. All the observations were carried out with the 1.5 m Carlos Sánchez telescope at the Observatorio del Teide. The instrumentation used consisted of a cooled broadband filters photometer with an InSb detector. The aperture size and the amplitude of the chopper were both 20 arcsec. The signal-to-noise ratio of the individual observations was always higher than 100. At the time of our observations, the infrared photometric system at the Observatorio del Teide was compatible with Johnson's system, except for a small discrepancy (less than 0.01 mag) in J (Arribas & Martínez-Roger 1987). In all the observing runs some measurements were also obtained with the H filter during the orbital phases of maxima.

BD+52°3375 was used as comparison star in all the observing runs. This star has never been used before, but it is easy to identify and also its spectral type is not very different to that of RT And. Standard stars of the Observatory were observed each night in order to check that the comparison star's brightness stayed the same. Within the errors of determination, the magnitudes of BD+52°3375 always remained constant during the different observation periods, and its calibrated magnitudes were

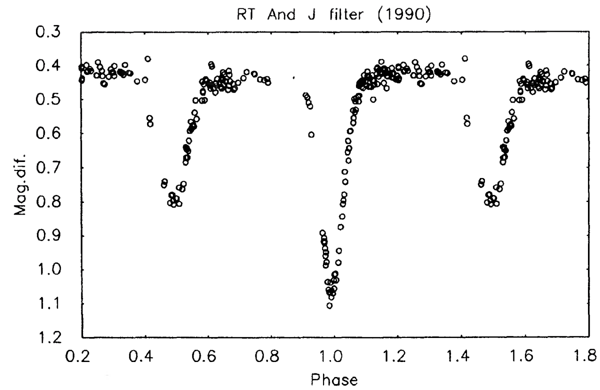

FIG. 1. Differential magnitude in the J filter for RT And in 1990. The comparison star is BD+52°3375.

$$J=7.40\pm0.01, \quad H=6.88\pm0.01, \quad K=6.74\pm0.01.$$

The BD+52°3375 color indices, $(J-K)=0.66$ and $(H-K)=0.14$, correspond to those of an unreddened K2−3 V star (Johnson 1966; Koornneef 1983), close to the spectral type K0 V given in the DM Catalogue.

Figures 1 and 2 give the 1990 differential magnitudes of RT And against orbital phase, in the J and K filters, respectively. Figures 3 and 4 represent the 1990, 1991, 1992, and 1994 observations in the J and K filters, superposed with different symbols. Tables 1 and 2 give the Heliocentric Julian Dates, differential magnitudes (RT And minus BD+52°3375) and the orbital phase values, for all the observations in the J and K filters, respectively. The orbital phase was calculated using the ephemeris given by Mancuso *et al.* (1979b), namely,

$$\mathrm{HJD}=2443732.4498+0\overset{\mathrm{d}}{.}6289296E. \tag{1}$$

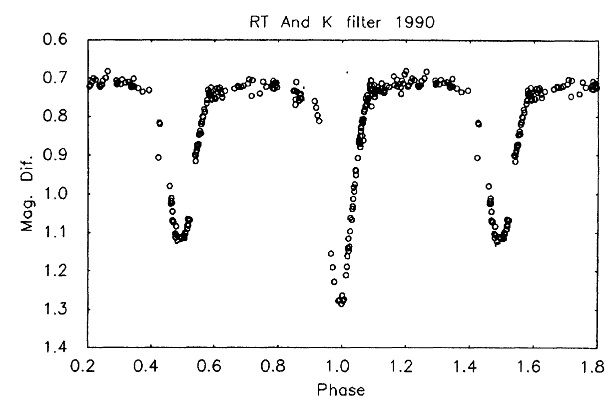

FIG. 2. Differential magnitude in the K filter for RT And in 1990. The comparison star is BD+52°3375.

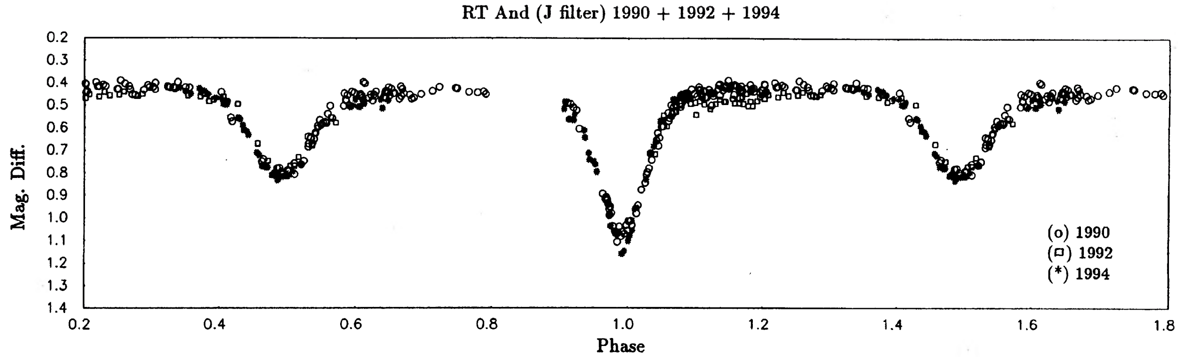

FIG. 3. Superposed differential magnitudes in the *J* filter for RT And in 1990, 1991, and 1994. The comparison star is BD+52°3375.

3. RESULTS AND DISCUSSION

3.1 Light Curves Variability

The light curve observed in 1990 August with the *J* filter (Fig. 1) presents an appreciable difference between the brightness of both its maxima. After the secondary eclipse the brightness seems to be depressed displaying narrow dips, which makes the maximum between phases 0.6 to 0.9 fainter than the other maximum by about 0.03 mag. This difference is unappreciable at longer wavelengths (*K* filter, Fig. 2), where the light curve is more regular. The visual light curves obtained contemporary to our IR observations, from October 3 to August 29 in U,B,V filters (Dapergolas *et al.* 1991), display a similar difference between the quadrature levels as noted in our *J* filter light curve, but it do not show any defined dips, which are probably transient features. Figures 3 and 4 show superposed all the IR observations taken throughout the different years. The most significant changes between the successive observations appear in the *J* filter, with a difference of about 0.04 mag. in the binary brightness after the primary minimum (orbital phases ~0.1–0.3), in the sense that during 1992 it was fainter than in 1990). A small narrow dip at phase ~0.3 is apparent the 1992 light curve. Once again, no significant variations are observed in the simultaneous *K* filter light curves. From the comparison of the observations taken along the years at the other maximum, orbital phases 0.6–0.8, no conclusions can be drawn since there are fewer points. The observations of the 1994 maxima do not display any appreciable features either in the *J* filter or in the *K* filter, and define a rather regular light curve.

Concerning the minima, the primary eclipse was observed twice, while the secondary was observed in three different years. As can be seen in Fig. 3, the *J* filter data show there are no differences in the observed depths of both minima at different epochs, with particularly good agreement in the secondary ones. Some differences (about 0.03 mag) were observed in the depth of the secondary minimum between the *K* filter light curves (Fig. 4).

As commented above, it is generally accepted that starspots are the main source of photometric variability in this active binary (Zeilik *et al.* 1989b). However, the well-defined depressions at the end of the 1990 secondary eclipse (Fig. 1), are too narrow to be interpreted as a cool starspot signature, suggesting the existence of a transient extinction effect, presumably associated to localized circumstellar structures on one or between both stars. Similar photometric depressions are frequently observed in many detached and semidetached binaries, particularly in the light curves at the beginning the end of the eclipses; we have observed them in the infrared in other short-period RS CVn systems (Arévalo & Lázaro 1990). Similar features in RT And visible light curves have been found before, at almost identical orbital phases (see Milano 1981), and in the 1964 light curves of Dean (1974), displaying variable absorption and emission at the end of the primary eclipse, with clear differences be-

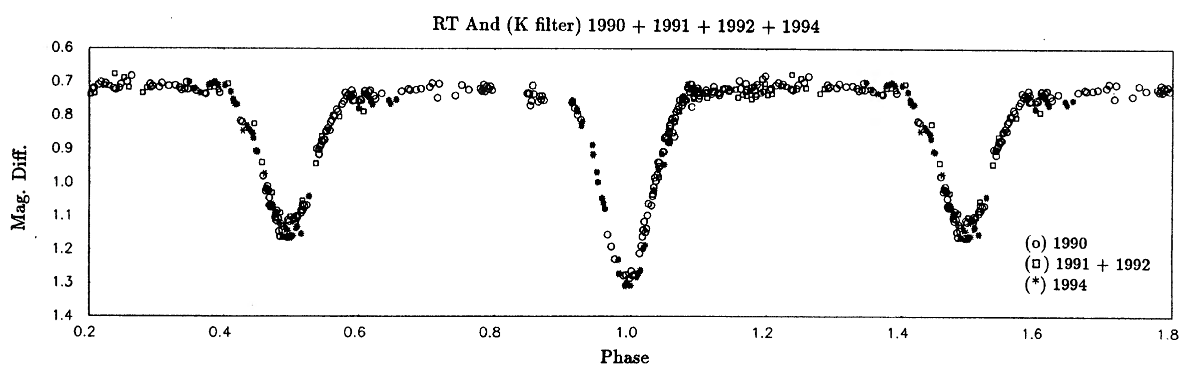

FIG. 4. Superposed differential magnitudes in the *K* filter for RT And in 1990, 1991, 1992, and 1994. The comparison star is BD+52°3375.

TABLE 1. *J* filter observations of RT And.

HJD	Phase	Δ J	HJD	Phase	Δ J	HJD	Phase	Δ J
2448113.602	0.045	0.679	2448113.611	0.060	0.569	2448113.616	0.068	0.531
2448113.622	0.078	0.506	2448113.623	0.079	0.489	2448113.626	0.084	0.447
2448113.632	0.094	0.429	2448113.635	0.098	0.448	2448113.645	0.114	0.463
2448113.646	0.116	0.463	2448113.651	0.123	0.442	2448113.652	0.125	0.446
2448113.657	0.134	0.410	2448113.659	0.136	0.455	2448113.668	0.151	0.412
2448113.672	0.156	0.452	2448113.677	0.165	0.468	2448113.679	0.167	0.413
2448113.680	0.169	0.433	2448113.687	0.181	0.435	2448113.689	0.183	0.426
2448113.690	0.186	0.422	2448113.701	0.202	0.444	2448113.702	0.204	0.438
2448114.464	0.416	0.555	2448114.465	0.418	0.572	2448114.493	0.462	0.750
2448114.494	0.465	0.740	2448114.505	0.481	0.803	2448114.507	0.485	0.780
2448114.512	0.493	0.807	2448114.523	0.510	0.758	2448114.536	0.530	0.685
2448114.538	0.534	0.647	2448114.544	0.544	0.592	2448114.547	0.549	0.588
2448114.569	0.583	0.447	2448114.570	0.585	0.475	2448114.576	0.594	0.440
2448114.578	0.597	0.445	2448114.584	0.606	0.458	2448114.585	0.609	0.457
2448114.598	0.629	0.439	2448114.607	0.644	0.468	2448114.610	0.648	0.442
2448114.621	0.666	0.416	2448114.623	0.668	0.428	2448114.630	0.679	0.454
2448114.640	0.696	0.450	2448114.650	0.712	0.437	2448114.657	0.722	0.419
2448114.672	0.746	0.424	2448114.673	0.748	0.425	2448114.684	0.766	0.441
2448114.692	0.779	0.443	2448114.698	0.788	0.440	2448114.700	0.791	0.451
2448115.508	0.076	0.493	2448115.508	0.076	0.490	2448115.511	0.080	0.459
2448115.515	0.087	0.445	2448115.526	0.105	0.430	2448115.528	0.107	0.446
2448115.536	0.120	0.444	2448115.544	0.133	0.425	2448115.545	0.135	0.405
2448115.554	0.149	0.425	2448115.555	0.151	0.421	2448115.563	0.164	0.423
2448115.564	0.166	0.431	2448115.570	0.174	0.424	2448115.574	0.181	0.408
2448115.584	0.197	0.430	2448115.585	0.199	0.432	2448115.587	0.202	0.404
2448115.597	0.217	0.398	2448115.598	0.219	0.418	2448115.606	0.231	0.416
2448115.617	0.250	0.430	2448115.620	0.254	0.390	2448115.629	0.268	0.431
2448115.630	0.271	0.452	2448115.633	0.275	0.455	2448115.652	0.305	0.401
2448115.664	0.324	0.420	2448115.666	0.326	0.422	2448115.670	0.334	0.427
2448115.680	0.350	0.421	2448115.684	0.355	0.422	2448115.697	0.377	0.447
2448115.713	0.402	0.442	2448115.719	0.411	0.380	2448117.464	0.186	0.437
2448117.470	0.195	0.442	2448117.474	0.202	0.407	2448117.486	0.222	0.415
2448117.490	0.228	0.409	2448117.503	0.249	0.429	2448117.510	0.260	0.405
2448117.514	0.266	0.416	2448117.528	0.288	0.433	2448117.532	0.294	0.411
2448117.533	0.296	0.420	2448117.550	0.323	0.417	2448117.555	0.331	0.421
2448117.560	0.338	0.398	2448118.549	0.911	0.488	2448118.551	0.915	0.494
2448118.554	0.919	0.510	2448118.557	0.924	0.521	2448118.560	0.928	0.604
2448118.582	0.963	0.892	2448118.584	0.967	0.917	2448118.585	0.969	0.922
2448118.588	0.973	0.987	2448118.591	0.979	1.036	2448118.599	0.990	1.081
2448118.602	0.995	1.070	2448120.472	0.968	0.907	2448120.473	0.970	0.916
2448120.474	0.971	0.937	2448120.474	0.973	0.959	2448120.475	0.974	0.949
2448120.477	0.976	0.978	2448120.480	0.982	1.059	2448120.481	0.983	1.067
2448120.482	0.985	1.106	2448120.483	0.986	1.066	2448120.484	0.988	1.038
2448120.487	0.992	1.062	2448120.490	0.998	1.031	2448120.491	1.000	1.056
2448120.492	0.001	1.014	2448120.494	0.004	1.012	2448120.495	0.006	1.031
2448120.500	0.013	0.979	2448120.501	0.015	0.944	2448120.504	0.020	0.874
2448120.508	0.026	0.843	2448120.509	0.027	0.807	2448120.510	0.029	0.796
2448120.511	0.031	0.779	2448120.513	0.033	0.712	2448120.514	0.035	0.742
2448120.518	0.042	0.655	2448120.519	0.044	0.622	2448120.521	0.046	0.644
2448120.523	0.049	0.594	2448120.524	0.052	0.593	2448120.529	0.059	0.533
2448120.530	0.061	0.555	2448120.531	0.063	0.499	2448120.532	0.065	0.538
2448120.534	0.067	0.506	2448120.535	0.070	0.495	2448120.540	0.077	0.460
2448120.541	0.079	0.452	2448120.543	0.081	0.453	2448120.544	0.083	0.452
2448120.545	0.085	0.455	2448120.546	0.087	0.463	2448120.548	0.089	0.448
2448120.549	0.091	0.467	2448120.556	0.102	0.458	2448120.557	0.105	0.418
2448120.559	0.107	0.433	2448120.560	0.109	0.463	2448120.561	0.111	0.434
2448120.563	0.113	0.439	2448120.567	0.120	0.429	2448120.568	0.121	0.445
2448120.569	0.123	0.500	2448120.571	0.126	0.457	2448120.580	0.140	0.433
2448120.581	0.141	0.414	2448120.582	0.143	0.421	2448120.582	0.144	0.411
2448120.584	0.146	0.424	2448120.585	0.148	0.389	2448120.590	0.156	0.411
2448120.591	0.157	0.408	2448120.592	0.160	0.413	2448121.427	0.488	0.778
2448121.429	0.491	0.796	2448121.435	0.500	0.789	2448121.436	0.502	0.791
2448121.441	0.510	0.806	2448121.447	0.520	0.763	2448121.450	0.524	0.747
2448121.454	0.531	0.671	2448121.456	0.534	0.643	2448121.458	0.536	0.670
2448121.459	0.539	0.651	2448121.461	0.541	0.621	2448121.465	0.547	0.566
2448121.466	0.550	0.585	2448121.468	0.552	0.577	2448121.469	0.555	0.575
2448121.471	0.557	0.579	2448121.472	0.558	0.539	2448121.474	0.562	0.503
2448121.476	0.565	0.557	2448121.487	0.582	0.503	2448121.489	0.585	0.480
2448121.490	0.587	0.455	2448121.492	0.591	0.502	2448121.502	0.606	0.450
2448121.504	0.609	0.468	2448121.505	0.611	0.396	2448121.506	0.613	0.402
2448121.510	0.619	0.467	2448121.512	0.622	0.453	2448121.513	0.624	0.479
2448121.514	0.626	0.452	2448121.515	0.628	0.459	2448121.524	0.641	0.463

TABLE 1. (continued)

HJD	Phase	Δ J	HJD	Phase	Δ J	HJD	Phase	Δ J
2448121.525	0.643	0.443	2448121.526	0.644	0.435	2448121.527	0.646	0.439
2448121.528	0.648	0.420	2448121.529	0.650	0.457	2448121.531	0.652	0.426
2448121.532	0.655	0.448	2448121.534	0.657	0.446	2448121.538	0.664	0.471
2448121.540	0.667	0.460	2448121.542	0.670	0.447	2448121.550	0.682	0.471
2448121.551	0.685	0.467	2448119.423	0.301	0.420	2448119.425	0.305	0.430
2448119.567	0.530	0.640	2448839.391	0.053	0.543	2448839.421	0.100	0.542
2448839.426	0.107	0.573	2448839.429	0.112	0.569	2448839.434	0.121	0.516
2448839.449	0.144	0.483	2448839.455	0.154	0.469	2448839.464	0.169	0.462
2448839.468	0.175	0.447	2448839.472	0.181	0.481	2448839.481	0.195	0.463
2448839.485	0.202	0.469	2448839.489	0.208	0.452	2448839.498	0.222	0.463
2448839.503	0.230	0.441	2448839.507	0.237	0.457	2448839.516	0.252	0.453
2448839.521	0.259	0.441	2448839.534	0.279	0.460	2448839.538	0.286	0.452
2448839.580	0.353	0.529	2448839.592	0.371	0.463	2448839.596	0.378	0.452
2448839.600	0.384	0.483	2448839.604	0.391	0.476	2448839.613	0.406	0.463
2448839.627	0.427	0.495	2448839.632	0.435	0.612	2448839.645	0.456	0.671
2448839.654	0.471	0.747	2448839.658	0.477	0.810	2448839.662	0.483	0.804
2448839.671	0.498	0.816	2448839.675	0.504	0.770	2448839.679	0.510	0.768
2448839.683	0.516	0.731	2448839.695	0.535	0.681	2448839.698	0.540	0.626
2448839.700	0.544	0.599	2448839.712	0.563	0.553	2448839.717	0.571	0.578
2448839.721	0.577	0.611	2448839.735	0.599	0.641	2448839.739	0.606	0.601
2448839.743	0.613	0.653	2448840.641	0.040	0.716	2448840.652	0.058	0.594
2448840.657	0.064	0.549	2448840.660	0.071	0.530	2448840.664	0.077	0.501
2448840.674	0.093	0.492	2448840.678	0.099	0.488	2448840.683	0.106	0.481
2448840.687	0.112	0.496	2448840.697	0.129	0.493	2448840.701	0.135	0.473
2448840.705	0.142	0.483	2448840.715	0.158	0.491	2448840.719	0.164	0.489
2448840.723	0.170	0.493	2448840.728	0.178	0.502	2448840.732	0.184	0.502
2448840.736	0.191	0.480	2448840.740	0.197	0.452	2449360.331	0.348	0.423
2449360.336	0.356	0.437	2449360.341	0.364	0.449	2449360.349	0.377	0.427
2449360.350	0.379	0.440	2449360.353	0.383	0.436	2449360.355	0.386	0.443
2449360.357	0.390	0.453	2449360.364	0.401	0.467	2449360.369	0.409	0.469
2449360.371	0.412	0.495	2449360.374	0.416	0.498	2449360.375	0.419	0.484
2449360.385	0.434	0.556	2449360.386	0.437	0.561	2449360.389	0.441	0.589
2449360.391	0.443	0.607	2449360.393	0.447	0.617	2449360.394	0.449	0.633
2449360.402	0.462	0.711	2449360.404	0.465	0.722	2449360.407	0.469	0.771
2449360.408	0.471	0.765	2449360.411	0.475	0.776	2449360.412	0.477	0.775
2449360.418	0.486	0.808	2449360.419	0.488	0.813	2449360.421	0.492	0.832
2449360.423	0.495	0.810	2449360.425	0.499	0.817	2449360.427	0.502	0.813
2449360.430	0.506	0.803	2449360.432	0.508	0.812	2449360.435	0.514	0.795
2449360.442	0.526	0.763	2449361.315	0.913	0.515	2449361.316	0.914	0.484
2449361.319	0.919	0.562	2449361.320	0.921	0.561	2449361.324	0.927	0.565
2449361.324	0.928	0.540	2449361.334	0.942	0.611	2449361.334	0.944	0.643
2449361.338	0.949	0.711	2449361.339	0.950	0.740	2449361.342	0.957	0.747
2449361.344	0.959	0.761	2449361.345	0.961	0.794	2449361.358	0.981	0.982
2449361.358	0.982	1.034	2449361.364	0.991	1.072	2449361.365	0.993	1.063
2449361.369	0.998	1.158	2449361.371	0.002	1.146	2449361.375	0.008	1.101
2449361.376	0.010	1.077	2449361.378	0.013	1.056	2449361.380	0.017	0.960
2449361.382	0.020	0.954	2449361.391	0.033	0.828	2449361.395	0.040	0.712
2449361.398	0.045	0.681	2449361.400	0.048	0.663	2449361.404	0.055	0.570
2449361.406	0.057	0.565	2449361.416	0.073	0.474	2449361.418	0.077	0.472
2449361.422	0.084	0.453	2449361.424	0.086	0.448	2449361.426	0.090	0.477
2449361.428	0.093	0.478	2449361.431	0.097	0.469	2449361.432	0.099	0.463
2449379.357	0.599	0.508	2449379.358	0.602	0.503	2449379.361	0.606	0.474
2449379.363	0.610	0.505	2449379.365	0.613	0.506	2449379.368	0.617	0.484
2449379.369	0.619	0.492	2449379.384	0.643	0.475	2449379.386	0.646	0.513

tween the ultraviolet, blue, and yellow light curves. Also the night-to-night fluctuations pointed out by Gordon (1955) and others are difficult to explain by the presence of spots, and their origin is most likely to be related to extinction and emission effects originated in extraphotospheric structures or in mass transfer processes (Piotrowski *et al.* 1974; Botsula 1985).

3.2 *Light Curves Solutions*

This section presents the solutions of the IR light curves, and the resulting parameters confronted with those obtained from previous determinations using visible light curves. The IR light curves of RT And in the J and K filters were analyzed by means of the set of programmes developed by Budding & Zeilik (1987). The limb-darkening coefficients were obtained by interpolation from Al-Naimy's (1978) tables. The accepted value for the mass ratio was $q=0.73$, as Popper (1994) determined using radial velocity curves. The eccentricity was assumed to be $e=0$, even though in some fits we assumed a value of $e=0.026$, as determined by Zeilik *et al.* (1989b), without significant variations in the resulting values. The mean stellar surface temperatures, used to calculate

TABLE 2. *K* filter observations of RT And.

HJD	Phase	Δ K	HJD	Phase	Δ K	HJD	Phase	Δ K
2448113.592	0.030	1.067	2448113.593	0.032	1.040	2448113.608	0.055	0.879
2448113.609	0.057	0.838	2448113.613	0.063	0.817	2448113.614	0.065	0.807
2448113.621	0.075	0.769	2448113.625	0.081	0.753	2448113.628	0.087	0.728
2448113.630	0.091	0.728	2448113.637	0.101	0.740	2448113.648	0.119	0.735
2448113.650	0.121	0.727	2448113.654	0.128	0.733	2448113.655	0.130	0.738
2448113.660	0.138	0.720	2448113.674	0.160	0.696	2448113.675	0.162	0.719
2448113.681	0.171	0.721	2448113.686	0.178	0.716	2448114.468	0.422	0.906
2448114.469	0.424	0.816	2448114.471	0.427	0.819	2448114.496	0.468	1.068
2448114.509	0.487	1.231	2448114.510	0.489	1.217	2448114.518	0.502	1.199
2448114.526	0.515	1.091	2448114.527	0.517	1.066	2448114.540	0.537	0.900
2448114.542	0.541	0.901	2448114.550	0.552	0.846	2448114.551	0.554	0.838
2448114.572	0.589	0.743	2448114.574	0.591	0.757	2448114.580	0.601	0.752
2448114.582	0.603	0.755	2448114.594	0.622	0.741	2448114.595	0.624	0.750
2448114.601	0.633	0.734	2448114.619	0.663	0.728	2448114.625	0.672	0.721
2448114.627	0.675	0.724	2448114.633	0.684	0.723	2448114.637	0.691	0.720
2448114.645	0.704	0.715	2448114.648	0.708	0.704	2448114.653	0.716	0.747
2448114.654	0.718	0.706	2448114.669	0.742	0.740	2448114.675	0.752	0.710
2448114.681	0.762	0.723	2448114.695	0.783	0.719	2448115.486	0.042	0.952
2448115.499	0.062	0.850	2448115.501	0.064	0.862	2448115.510	0.079	0.752
2448115.511	0.080	0.754	2448115.517	0.090	0.774	2448115.519	0.093	0.731
2448115.523	0.100	0.749	2448115.538	0.124	0.727	2448115.543	0.131	0.732
2448115.547	0.138	0.719	2448115.552	0.146	0.723	2448115.567	0.170	0.704
2448115.576	0.184	0.741	2448115.577	0.186	0.707	2448115.582	0.194	0.690
2448115.589	0.205	0.722	2448115.591	0.207	0.718	2448115.595	0.214	0.709
2448115.609	0.237	0.719	2448115.611	0.240	0.723	2448115.616	0.247	0.707
2448115.644	0.292	0.717	2448115.645	0.295	0.712	2448115.654	0.308	0.704
2448115.660	0.318	0.712	2448115.672	0.337	0.724	2448115.677	0.344	0.701
2448115.678	0.346	0.722	2448115.686	0.358	0.726	2448115.695	0.373	0.736
2448115.707	0.393	0.732	2448117.462	0.183	0.724	2448117.466	0.190	0.715
2448117.472	0.199	0.681	2448117.484	0.218	0.701	2448117.488	0.225	0.705
2448117.501	0.245	0.718	2448117.508	0.257	0.700	2448117.512	0.263	0.683
2448117.530	0.291	0.706	2448117.538	0.304	0.716	2448117.553	0.328	0.710
2448117.557	0.335	0.717	2448117.562	0.342	0.721	2448118.550	0.913	0.760
2448118.553	0.917	0.777	2448118.555	0.921	0.797	2448118.559	0.926	0.812
2448118.583	0.965	1.155	2448118.587	0.971	1.191	2448118.590	0.976	1.229
2448118.598	0.989	1.277	2448118.600	0.992	1.276	2448118.604	0.998	1.285
2448118.605	0.001	1.264	2448118.606	0.002	1.277	2448118.607	0.004	1.276
2448118.609	0.006	1.274	2448118.613	0.012	1.211	2448118.614	0.015	1.189
2448118.615	0.017	1.161	2448118.616	0.018	1.141	2448118.617	0.019	1.116
2448118.618	0.021	1.149	2448118.619	0.023	1.137	2448118.620	0.024	1.097
2448118.621	0.025	1.062	2448118.625	0.032	1.033	2448118.626	0.033	1.013
2448118.627	0.035	0.984	2448118.628	0.037	0.994	2448118.629	0.038	0.976
2448118.630	0.040	0.939	2448118.631	0.042	0.940	2448118.634	0.047	0.908
2448118.635	0.048	0.908	2448118.636	0.050	0.867	2448118.637	0.051	0.863
2448118.638	0.052	0.861	2448118.639	0.054	0.870	2448118.640	0.056	0.851
2448118.641	0.057	0.828	2448118.642	0.058	0.830	2448118.642	0.060	0.812
2448118.643	0.061	0.808	2448118.647	0.067	0.787	2448118.648	0.069	0.782
2448118.649	0.070	0.772	2448118.650	0.072	0.754	2448118.652	0.075	0.760
2448118.653	0.077	0.745	2448118.654	0.078	0.744	2448118.658	0.084	0.716
2448118.658	0.085	0.719	2448118.659	0.087	0.730	2448118.660	0.088	0.706
2448118.661	0.090	0.707	2448118.662	0.091	0.719	2448118.663	0.093	0.741
2448118.666	0.097	0.735	2448118.667	0.099	0.718	2448118.668	0.101	0.732
2448118.674	0.109	0.732	2448118.675	0.111	0.723	2448118.676	0.113	0.731
2448118.681	0.121	0.728	2448118.682	0.122	0.713	2448119.522	0.458	0.980
2448119.524	0.462	1.025	2448119.525	0.463	1.018	2448119.526	0.464	1.011
2448119.527	0.466	1.024	2448119.528	0.468	1.046	2448119.529	0.469	1.073
2448119.530	0.470	1.071	2448119.530	0.471	1.072	2448119.533	0.476	1.104
2448119.534	0.478	1.113	2448119.535	0.479	1.084	2448119.536	0.480	1.107
2448119.537	0.482	1.146	2448119.538	0.483	1.162	2448119.539	0.485	1.124
2448119.540	0.486	1.141	2448119.541	0.488	1.132	2448119.544	0.493	1.164
2448119.545	0.495	1.112	2448119.546	0.497	1.116	2448119.548	0.499	1.161
2448119.550	0.503	1.108	2448119.551	0.505	1.110	2448119.552	0.506	1.115
2448119.553	0.507	1.100	2448119.554	0.509	1.104	2448119.558	0.515	1.082
2448119.559	0.517	1.083	2448119.561	0.520	1.070	2448119.563	0.523	1.068
2448119.574	0.541	0.916	2448119.575	0.542	0.894	2448119.576	0.544	0.888
2448119.576	0.545	0.874	2448119.577	0.546	0.879	2448119.578	0.548	0.872
2448119.579	0.549	0.872	2448119.580	0.551	0.848	2448119.584	0.557	0.844
2448119.585	0.558	0.820	2448119.586	0.560	0.814	2448119.587	0.562	0.800
2448119.588	0.564	0.802	2448119.590	0.567	0.782	2448119.591	0.569	0.789
2448119.595	0.575	0.766	2448119.597	0.577	0.758	2448119.598	0.580	0.732
2448119.600	0.582	0.743	2448119.601	0.584	0.737	2448119.603	0.587	0.745
2448119.604	0.589	0.725	2448119.606	0.591	0.737	2448119.607	0.593	0.754
2448119.616	0.608	0.727	2448119.618	0.611	0.737	2448119.620	0.614	0.730

TABLE 2. (continued)

HJD	Phase	Δ K	HJD	Phase	Δ K	HJD	Phase	Δ K
2448119.621	0.616	0.725	2448119.723	0.779	0.720	2448119.725	0.781	0.727
2448119.727	0.784	0.708	2448119.728	0.786	0.728	2448119.730	0.788	0.713
2448119.731	0.791	0.721	2448119.733	0.793	0.713	2448119.734	0.796	0.725
2448121.653	0.847	0.734	2448121.655	0.849	0.733	2448121.656	0.851	0.734
2448121.657	0.852	0.770	2448121.657	0.854	0.756	2448121.659	0.856	0.710
2448121.660	0.857	0.736	2448121.664	0.864	0.759	2448121.665	0.866	0.743
2448121.666	0.868	0.752	2448121.667	0.869	0.741	2448121.669	0.872	0.754
2448265.419	0.435	0.845	2448265.424	0.442	0.932	2448265.429	0.450	0.854
2448265.440	0.468	0.974	2448265.444	0.475	1.029	2448265.454	0.491	1.121
2448265.458	0.498	1.131	2448265.462	0.503	1.145	2448265.465	0.508	1.119
2448839.391	0.053	1.042	2448839.422	0.101	0.779	2448839.426	0.108	0.804
2448839.429	0.113	0.846	2448839.435	0.122	0.770	2448839.449	0.144	0.727
2448839.455	0.155	0.721	2448839.464	0.169	0.728	2448839.468	0.175	0.725
2448839.472	0.181	0.712	2448839.481	0.195	0.727	2448839.485	0.202	0.737
2448839.489	0.208	0.734	2448839.498	0.223	0.711	2448839.503	0.230	0.712
2448839.508	0.238	0.677	2448839.517	0.252	0.689	2448839.521	0.259	0.717
2448839.534	0.280	0.733	2448839.538	0.286	0.718	2448839.581	0.354	0.781
2448839.592	0.372	0.735	2448839.596	0.378	0.717	2448839.600	0.385	0.716
2448839.604	0.391	0.724	2448839.614	0.406	0.705	2448839.618	0.414	0.758
2448839.632	0.436	0.962	2448839.638	0.445	0.825	2448839.645	0.456	0.940
2448839.655	0.471	1.030	2448839.659	0.478	1.098	2448839.662	0.484	1.090
2448839.672	0.499	1.102	2448839.675	0.504	1.107	2448839.679	0.510	1.101
2448839.683	0.516	1.054	2448839.695	0.536	0.944	2448839.698	0.541	0.902
2448839.701	0.545	0.863	2448839.713	0.563	0.801	2448839.717	0.571	0.804
2448839.721	0.578	0.852	2448839.735	0.600	0.758	2448839.740	0.606	0.788
2448839.744	0.613	0.814	2448840.642	0.041	0.983	2448840.653	0.058	0.847
2448840.657	0.065	0.817	2448840.661	0.071	0.788	2448840.665	0.077	0.762
2448840.675	0.093	0.748	2448840.679	0.100	0.731	2448840.683	0.106	0.734
2448840.687	0.113	0.746	2448840.697	0.129	0.732	2448840.701	0.136	0.719
2448840.706	0.142	0.717	2448840.715	0.158	0.745	2448840.719	0.164	0.737
2448840.723	0.171	0.739	2448840.728	0.178	0.750	2448840.732	0.185	0.737
2448840.736	0.191	0.733	2448840.740	0.198	0.705	2449360.331	0.348	0.700
2449360.336	0.357	0.720	2449360.341	0.364	0.732	2449360.349	0.377	0.709
2449360.351	0.380	0.706	2449360.353	0.384	0.706	2449360.355	0.386	0.700
2449360.358	0.391	0.709	2449360.364	0.401	0.710	2449360.369	0.410	0.729
2449360.372	0.413	0.751	2449360.374	0.417	0.767	2449360.375	0.419	0.766
2449360.385	0.434	0.832	2449360.387	0.437	0.841	2449360.389	0.441	0.850
2449360.391	0.444	0.867	2449360.393	0.447	0.906	2449360.395	0.450	0.907
2449360.403	0.462	1.018	2449360.405	0.466	1.025	2449360.407	0.470	1.068
2449360.409	0.472	1.065	2449360.411	0.476	1.090	2449360.412	0.478	1.088
2449360.418	0.487	1.162	2449360.419	0.489	1.164	2449360.422	0.493	1.140
2449360.423	0.495	1.165	2449360.426	0.499	1.165	2449360.428	0.502	1.159
2449360.431	0.507	1.137	2449360.432	0.509	1.133	2449360.435	0.514	1.153
2449360.443	0.526	1.041	2449361.315	0.913	0.757	2449361.316	0.914	0.755
2449361.319	0.920	0.779	2449361.320	0.921	0.787	2449361.324	0.927	0.829
2449361.325	0.928	0.818	2449361.334	0.943	0.887	2449361.335	0.944	0.916
2449361.338	0.949	0.968	2449361.339	0.951	0.998	2449361.343	0.957	1.045
2449361.344	0.959	1.060	2449361.346	0.962	1.077	2449361.358	0.981	1.230
2449361.359	0.982	1.272	2449361.364	0.991	1.308	2449361.366	0.994	1.299
2449361.369	0.999	1.307	2449361.371	0.002	1.342	2449361.375	0.008	1.282
2449361.376	0.011	1.272	2449361.378	0.014	1.261	2449361.381	0.017	1.197
2449361.383	0.020	1.188	2449361.391	0.034	1.022	2449361.395	0.040	0.961
2449361.399	0.046	0.915	2449361.400	0.049	0.946	2449361.404	0.055	0.842
2449361.406	0.058	0.880	2449361.417	0.074	0.750	2449361.418	0.077	0.742
2449361.423	0.084	0.706	2449361.424	0.087	0.719	2449361.427	0.091	0.714
2449361.428	0.093	0.724	2449361.431	0.097	0.729	2449361.432	0.100	0.722
2449379.357	0.600	0.778	2449379.361	0.606	0.734	2449379.364	0.611	0.736
2449379.365	0.613	0.745	2449379.368	0.617	0.757	2449379.370	0.620	0.768
2449379.385	0.644	0.755	2449379.386	0.646	0.764	2449379.392	0.655	0.752

the gravity darkening exponents, were T_1=6100 K and T_2=4900 K, according to the values of Straizys & Kuriliene (1981) for the spectroscopic classification of the primary and secondary components of RT And, F8−G0 V and K0−2 V, respectively. The adopted values for the effective temperatures of the stars do not have an appreciable affect on the fitted parameters, i.e., the relative luminosities and radii of the components, are within a range of at least ±300 K, and so a moderate error in the assumed values does not determine the results of the light curve analysis.

We have searched in the literature for previous solutions to other light curves, and it is interesting to summarize here the results obtained from visual photometry. Detailed analyses of visual light curve parameters have been performed by

TABLE 3. Results from previous photometric solutions at *V* filter light curves of RT And.

	References							
Parameters	1 1944	2 1962	3 1973	4 1978	5 1949--1978	6 1978	7 1981	8 1987
k=r$_2$/r$_1$....	0.52	0.738	0.696	0.887	0.715	0.871	0.723	0.722
r$_1$		0.316	0.331	0.301	0.324	0.287	0.311	0.315
r$_2$		0.234	0.230	0.267	0.232	0.250	0.225	0.227
i	82.7	87.6	87.3	80.9	87.3	82.0	88.9	88.4
L$_1$	0.63	0.818	0.853	0.776	0.880	0.83	0.857	0.895
L$_2$	0.37	0.182	0.147	0.224	0.120	0.17	0.143	0.105
e	0.089		0.08					0.026
Espec. type$_1$	G0	F8V	F8V	F8V	F8V	F8V	F8V	F8V
Espec. type$_2$	K1	G5V	K0V	K0V			K0V	K0V

References: (1) Payne–Gaposchkin 1946. (2) Dean 1974. (3) Dumistrescu 1973. (4) Mancuso *et al.* 1979. (5) Milano *et al.* 1981. (6) Mancuso *et al.* 1981. (7) Budding y Zeilik 1987. (8) Zeilik *et al* 1989.

different authors. Milano *et al.* (1981) conducted an homogeneous analysis of ten light curves obtained for RT And (from 1949 to 1978), employing two different fitting programmes: Wood's (1971, 1972) and Wilson & Devinney's (1971) models, and inferred an unique solution for all the light curves, which is given in Table 3. In a more recent work, Zeilik *et al.* (1989b), by means of a different fitting programme (Budding & Zeilik 1987), examined an extensive sample of published *V* light curves, removing the contribution of cool starspots, and inferred similar values for the geometrical parameters (also given in Table 3) as reported by Milano *et al.* (1981). This result is important because it indicates that the obtained geometrical parameters do not depend on the method utilized to derive the light curve solutions. The results from other existing determinations are also provided in the same table, but note that some of the values of the reported parameters are now rather different. In general, two values for the orbital inclination are available from the light curves analyses published: around 82° or 88°, and the radii ratio $k=r_2/r_1$ takes the alternative values approximately 0.88 or 0.72.

In the analysis of our IR light curves, we adopted two sets of values as initial parameters, using the most different sets of solutions obtained from previous determinations via visual photometry, namely, the values obtained by Mancuso *et al.* (1981) and those determined by Zeilik *et al.* (1989b). Two solutions, a and b (given in Tables 4 and 5), represent the best fits obtained when the first or second set of values for the geometrical parameters are taken respectively as starting points in the fitting procedure. Both solutions a and b fit the

TABLE 4. Results of solution a.

J Filter 1990	J Filter (*) 1990	K Filter 1990	J Filter 1990 + 1994	K Filter 1990 + 1994
L$_1$=0.633 ± 0.002	L$_1$=0.640 ± 0.002	L$_1$=0.609 ± 0.002	L$_1$=0.664 ± 0.002	L$_1$=0.632 ± 0.002
L$_2$=0.367 ± 0.002	L$_2$=0.359 ± 0.002	L$_2$=0.391 ± 0.002	L$_2$=0.337 ± 0.002	L$_2$=0.367 ± 0.002
r$_1$=0.291 ± 0.001	r$_1$=0.305 ± 0.001	r$_1$=0.297 ± 0.001	r$_1$=0.302 ± 0.001	r$_1$=0.300 ± 0.001
r$_2$=0.270 ± 0.001	r$_2$=0.276 ± 0.001	r$_2$=0.266 ± 0.001	r$_2$=0.262 ± 0.001	r$_2$=0.259 ± 0.001
i=82°	i=82°	i=82°	i=82°	i=82°
T$_1$=6100 K	T$_1$=6100 K	T$_1$=6100 K	T$_1$=6100 K	T$_1$=6100 K
T$_2$=4900 K	T$_2$=4900 K	T$_2$=4900 K	T$_2$=4900 K	T$_2$=4900 K
χ^2=567	χ^2=516	χ^2=490	χ^2=460	χ^2=500
ϵ=0.016	ϵ=0.015	ϵ=0.014	ϵ=0.013	ϵ=0.013

(*) Only data points of the brightess maximum (orbital phases 0.1–0.4.) were considered in the fit.

TABLE 5. Results of solution b.

J Filter 1990	J Filter (*) 1990	K Filter 1990	J Filter 1990 + 1994	K Filter 1990 + 1994
L_1=0.746 ± 0.002	L_1=0.743 ± 0.002	L_1=0.731 ± 0.002	L_1=0.742 ± 0.002	L_1=0.712 ± 0.002
L_2=0.254 ± 0.002	L_2=0.257 ± 0.002	L_2=0.269 ± 0.002	L_2=0.258 ± 0.002	L_2=0.288 ± 0.002
r_1=0.318 ± 0.001	r_1=0.320 ± 0.001	r_1=0.317 ± 0.001	r_1=0.318 ± 0.001	r_1=0.307 ± 0.001
r_2=0.226 ± 0.001	r_2=0.233 ± 0.001	r_2=0.218 ± 0.001	r_2=0.232 ± 0.001	r_2=0.221 ± 0.001
i=87°	i=87°	i=87°	i=87°	i=87°
T_1=6100 K	T_1=6100 K	T_1=6100 K	T_1=6100 K	T_1=6100 K
T_2=4900 K	T_2=4900 K	T_2=4900 K	T_2=4900 K	T_2=4900 K
χ^2=567	χ^2=516	χ^2=490	χ^2=460	χ^2=500
ϵ=0.016	ϵ=0.015	ϵ=0.014	ϵ=0.013	ϵ=0.013

(*) Only data points of the brightess maximum (orbital phases 0.1–0.4.) were considered in the fit.

J and *K* light curves satisfactorily, in agreement with the results based on visible light curves, but the depth of the secondary eclipse is better reproduced in solution b. In order to check if there are other local minima in the fitting process, we have tried using other initial sets for the values of the free parameters. The conclusion of this parametric search is that the radii ratio $k=0.70$ (solution b) is the minimum value that fits satisfactorily our IR light curves, and the undetermination between solutions a and b still remains. Different fits were carried out for the 1990 *J* and *K* filters light curves, and also for the *J* and *K* combined observations of 1990 and 1994 runs. Tables 4 and 5 give the values obtained in the *J* and *K* light curve solutions, both for the 1990 data and for the combined 1990 plus 1994 observations. Figures 5 to 8 represent the theoretical models superposed to the observations for these fits. In both cases (a and b), in the analysis of the *J* filter 1990 light curve, we attempted to find solutions by assuming that the maximum between orbital phase values 0.1–0.4 represents the brightness of the unperturbed stars, removing the points of the lower maximum, but this restriction only yields very slight changes in the resulting elements, also listed in Tables 4 and 5.

3.3 Colors, Spectral Types and Effective Temperatures of the Stellar Components and Distance to RT And

Even though RT And has been observed extensively, most of its visual light curves have not been calibrated in the standard photometric system. The visual photometry carried out by Dapergolas *et al.* (1991) encompasses the most contemporary measurements to our 1990 infrared photometry, but their visual light curves are given in differential magnitudes relative to BD+52°3384, chosen as comparison star. Recently, Heckert (1994) determined for us the following standard magnitudes for this comparison star: $U=10.96$, $B=10.25$, $V=10.12$, $R=10.05$, and $I=9.99$. Using this calibration of the comparison star and the differential *B*, *V* photometry provided by Dapergolas *et al.* (1991), we calculated the magnitudes and colours for RT And given in Table 6. RT And is a relatively close system (about 103 pc, see later) and the interstellar extinction towards its galactic coordinates, $l=108.06°$ and $b=-6.93°$, seems not to be important (Lynds 1962), so we assumed that interstellar reddening does not affect the observed colors.

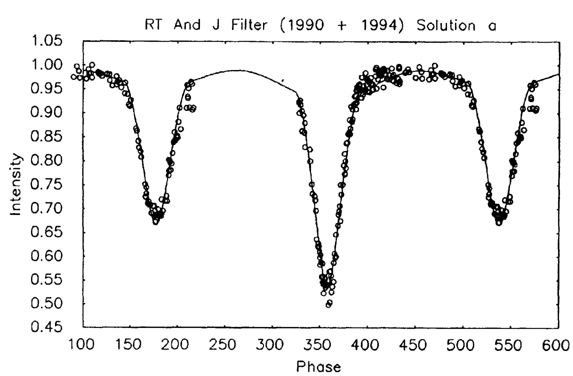

FIG. 5. Theoretical light curve from solution a together with the observations (*J* filter). Only the brightest maximum was considered.

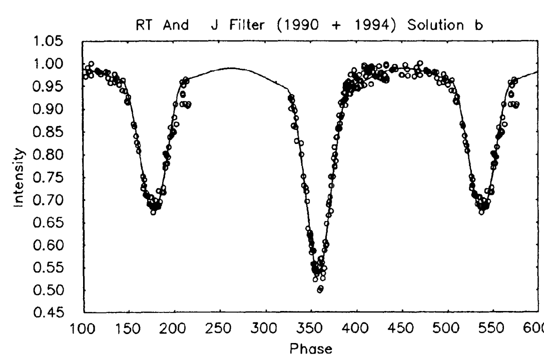

FIG. 6. Theoretical light curve from solution b together with the observations (*J* filter). Only the brightness maximum was considered.

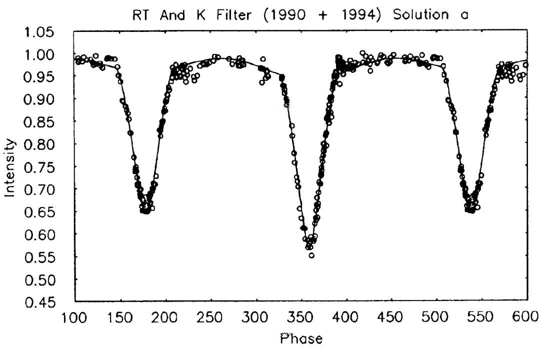

FIG. 7. Theoretical light curve from solution a together with the observations (K filter).

3.3.1 *The spectral types of the components of RT And based on the depths of the observed eclipses*

We can relate the color $(\lambda_i-\lambda_j)^{(b)}$ of a binary measured out of eclipses with the color of the primary or secondary component, $(\lambda_i-\lambda_j)^{(1),(2)}$, and the partial contribution of the component star to the total light of the system by the expression:

$$(\lambda_i-\lambda_j)^{(b)}=(\lambda_i-\lambda_j)^{(1),(2)}-2.5\ \log(L_{\lambda_j}^{(1),(2)}/L_{\lambda_i}^{(1),(2)}), \tag{2}$$

where $L_{\lambda_i}^{(1),(2)}$ is the partial contribution of the primary or secondary star to the total brightness in the filter λ_i and $L_{\lambda_j}^{(1),(2)}$ its the partial contribution in λ_j. We can use relation (2) to deduce the separate colors of the primary and secondary components of RT And, in order to check its agreement with those expected from their spectroscopic classification. We applied relation (2) with the colors $(V-J)$ and $(V-K)$ measured at maxima (Table 6), while for $L_J^{(1),(2)}$ and $L_K^{(1),(2)}$ we use the values obtained from solutions a and b to the J and K light curves, and for $L_V^{(1),(2)}$ we adopt Mancuso *et al.*'s (1979) values for case a and Budding & Zeilik's (1987) for case b (Table 3), as those solutions to the V light curves yield parameters very close to our a and b solutions respectively. We obtain for the two possible solutions:

Case a: Primary star: $(V-J)^{(1)}=0.96$, $(V-K)^{(1)}=1.28$. Secondary star: $(V-J)^{(2)}=1.68$, $(V-K)^{(2)}=2.15$.

Comparing these values with Johnson's (1966) colors for normal stars, the derived colors of the primary component agree very well with those typical of F8 V stars, while the derived colors for the secondary component correspond to K2 V stars.

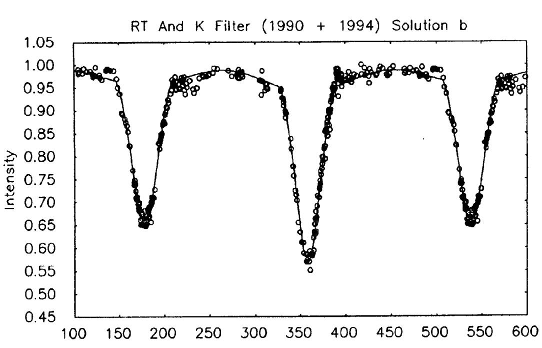

FIG. 8. Theoretical light curve from solution b together with the observations (K filter).

TABLE 6. $(V-\lambda)$ observed colors of RT And.

V−λ	Maxima	Primary Minimum	Secondary Minimum
V−B	−0.53	−0.58	−0.49
V−J	1.17	1.36	1.08
V−H	1.43	–	–
V−K	1.54	1.80	1.39

Case b: Primary star: $(V-J)^{(1)}=1.01$, $(V-K)^{(1)}=1.37$. Secondary star: $(V-J)^{(2)}=1.80$, $(V-K)^{(2)}=2.23$.

Now the derived colors of the primary component indicate a G0 V type, while the derived colors for the secondary component correspond to a type slightly later than K2 V.

For both stellar components the derived colours are somewhat redder accepting solution b to the light curves instead of solution a, but in any case similar to the spectroscopic classifications F8 V−G0 V for the primary star, and about K2 V for the secondary, indicating that the visual-near-infrared fluxes resemble rather well that of normal stars, without any appreciable IR excess.

3.3.2 *The spectral types of the components of RT And by comparison between the colors measured out of eclipse with those expected from a pair of normal stars*

In order to effect the comparison we need a reference of the expected colors for a binary system composed by two normal stars. We use as a reference the synthetic colors obtained after combining two stars with similar spectral types to those determined from spectroscopic observations of RT And, with radii determined from the photometric light curve solutions, and using the empirical visual surface brightness-spectral type relation. The expected colors $(m_{\lambda_i}-m_{\lambda_j})$ out of eclipses are calculated by the expression:

$$(m_{\lambda_i}-m_{\lambda_j})^{(b)} =-2.5\ \log \times\left(\frac{F_V^{(1)}r_{(1)}^2 10^{0.4(V-\lambda_i)^{(1)}}+F_V^{(2)}r_{(2)}^2 10^{0.4(V-\lambda_i)^{(2)}}}{F_V^{(1)}r_{(1)}^2 10^{0.4(V-\lambda_j)^{(1)}}+F_V^{(2)}r_{(2)}^2 10^{0.4(V-\lambda_j)^{(2)}}}\right), \tag{3}$$

where F_V is the stellar surface brightness in the V band, r the stellar relative radius and $(V-\lambda)$ the color, with the indices (1) and (2) for the primary and secondary stars, respectively. The colors for the stellar components of RT And were taken from Johnson's (1966) tables of average colors for normal stars of the assumed spectral types, those spectroscopically determined for the components of RT And; for the surface brightness in the visual band F_V, we adopted Eaton & Poe's (1984) values, from a redetermination of the empirical surface brightness–color relation for main-sequence spectral types; for the stellar relative radii, we used the values from the light curve solutions of the present work, employing the

TABLE 7. Predicted colors out of the eclipses and primary star contributions to the total light for the combination of two stars with spectral types indicated. Normal colors from Johnson (1966) and visual surface brightness from Eaton & Poe (1984).

	Solution a			**Solution b**		
F8V + K0V	B−V=0.606	V−J=1.086	V−K=1.445	B−V=0.584	V−J=1.046	V−K=1.391
	$L_V{}^1$=0.74	$L_J{}^1$=0.66	$L_K{}^1$=0.63	$L_V{}^1$=0.825	$L_J{}^1$=0.762	$L_K{}^1$=0.74
F8V + K2V	B−V=0.599	V−J=1.097	V−K=1.448	B−V=0.578	V−J=1.051	V−K=1.417
	$L_V{}^1$=0.82	$L_J{}^1$=0.72	$L_K{}^1$=0.67	$L_V{}^1$=0.88	$L_J{}^1$=0.81	$L_K{}^1$=0.77
F8V + K5V	B−V=0.582	V−J=1.112	V−K=1.517	B−V=0.566	V−J=1.058	V−K=1.432
	$L_V{}^1$=0.912	$L_J{}^1$=0.79	$L_K{}^1$=0.73	$L_V{}^1$=0.94	$L_J{}^1$=0.86	$L_K{}^1$=0.81
G0V + K0V	B−V=0.651	V−J=1.142	V−K=1.511	B−V=0.631	V−J=1.108	V−K=1.462
	$L_V{}^1$=0.71	$L_J{}^1$=0.64	$L_K{}^1$=0.61	$L_V{}^1$=0.80	$L_J{}^1$=0.75	$L_K{}^1$=0.72
G0V + K2V	B−V=0.648	V−J=1.161	V−K=1.563	B−V=0.628	V−J=1.118	V−K=1.495
	$L_V{}^1$=0.80	$L_J{}^1$=0.71	$L_K{}^1$=0.66	$L_V{}^1$=0.87	$L_J{}^1$=0.80	$L_K{}^1$=0.76
G0V + K5V	B−V=0.635	V−J=1.185	V−K=1.603	B−V=0.618	V−J=1.130	V−K=1.560
	$L_V{}^1$=0.90	$L_J{}^1$=0.78	$L_K{}^1$=0.71	$L_V{}^1$=0.94	$L_J{}^1$=0.85	$L_K{}^1$=0.80

values obtained from solutions a and b (Tables 4 and 5). The expected colors calculated using expression (3) for certain combinations of spectral types, with the partial contribution of the primary star in V, J, and K, are given in Table 7.

The comparison between RT And's observed colors and those expected from the combination of a F8−G0 V primary and a K0−5 V secondary, indicates that the observed $(B-V)$ color of RT And at maxima is bluer than expected. In fact the measured $(B-V)$ corresponds to a combined spectral type F8 V. Some blue excess in the $(B-V)$ color is normal in active stars and hence it is not a good indicator of the spectral types of the stars. The predicted $(V-J)$ and $(V-K)$ colors are too blue if the primary is a F8 V type, and the partial contributions of the primary star to the total light is too high if the secondary is later than K2 V. The spectral types of the components G0 V and K2 V give the best agreement between the predicted and observed colors. If we consider the colors measured during the secondary eclipse, an occultation in the solution b (we will argue that this must be accepted as the correct one), while the measured $(B-V)$ color is between those typical of F5 V and F8 V stars, the $(V-J)$ and $(V-K)$ colors would better correspond to a G0 −1 V spectral type for the primary star, based on Johnson's (1966) tabulation of normal colors. This result is compatible with that of the previous estimation for solution b, based in a different method. Then, the colors out of eclipses and at the secondary minimum point to a primary star slightly redder than expected from the spectroscopic classification. However, given the intrinsic dispersion in observed colors for stars of identical spectral type, and that the visual and infrared photometry are not simultaneous, the small disagreement between the expected and measured colors cannot be considered significant.

3.3.3 The effective temperatures of RT And's components and the distance to the system

We use the separate $(V-K)$ colors of the RT And's components derived from relation (2), to estimate the $T_{\rm eff}$ of the stars. The $(V-K)$ color is a good temperature indicator, and relatively unsensitive to other variables such as the composition or surface gravities. We have used the calibration $(V-K)-T_{\rm eff}$ from Alonso *et al.* (1995), based on the application of the infrared flux method and the new ATLAS model atmospheres (Kurucz 1991). For solar abundances, the calibration gives $\theta_{\rm eff}=5040./T_{\rm eff}=0.555+0.195(V-K)+0.0131(V-K)^2$. Then, for both cases a and b, we have

Case a: $(V-K)^{(1)}=1.28$: $T_{\rm eff}^{(1)}=6100$ K,

$(V-K)^{(2)}=2.15$: $T_{\rm eff}^{(2)}=4960$ K.

Case b: $(V-K)^{(1)}=1.37$: $T_{\rm eff}^{(1)}=5950$ K,

$(V-K)^{(2)}=2.23$: $T_{\rm eff}^{(2)}=4880$ K.

As in case b the secondary eclipse is a total one, we could use the value $(V-K)=1.39$ directly, measured at the secondary minimum (Table 6), as the intrinsic color of the primary star to derive: $T_{\rm eff}^{(1)}=5920$ K. The estimated uncertainties in $T_{\rm eff}$ are ±100 K for the primary star and ±50 K for the secondary component.

The $T_{\rm eff}$ values derived from the $(V-K)$ colors are in good agreement with those reported by Popper (1980) and

TABLE 8. Predicted magnitudes out of eclipses and primary star contribution to the total light, for the combination of two ATLAS model atmospheres with T_{eff} indicated and the radii from our light curves solutions. The distance has been adjusted to give $V=8.99$, the observed visible magnitude of maxima.

Solution a

Tef. (1) (K)	Tef. (2) (K)	D (pc)	B	V	J	H	K
6000 +	4500	97.5	9.619	8.994	7.768	7.386	7.315
	4750	100.5	9.629	8.996	7.782	7.421	7.353
	5000	103.7	9.627	8.991	7.799	7.460	7.394
	5250	107.5	9.621	8.989	7.828	7.508	7.446
	5500	112.0	9.613	8.993	7.871	7.569	7.510
6250 +	4500	105.5	9.547	8.990	7.873	7.523	7.451
	4750	108.4	9.560	8.994	7.883	7.552	7.483
	5000	111.5	9.565	8.992	7.897	7.585	7.518
	5250	115.0	9.563	8.989	7.917	7.623	7.560
	5500	119.0	9.556	8.989	7.947	7.670	7.610

Solution b

Tef. (1) (K)	Tef. (2) (K)	D (pc)	B	V	J	H	K
6000 +	4500	99.0	9.595	8.989	7.827	7.479	7.413
	4750	101.0	9.602	8.990	7.834	7.500	7.436
	5000	103.5	9.609	8.994	7.851	7.532	7.470
	5250	106.0	9.604	8.991	7.868	7.562	7.503
	5500	109.0	9.597	8.991	7.894	7.602	7.544
6250 +	4500	108.0	9.533	8.994	7.942	7.628	7.561
	4750	109.7	9.537	8.992	7.942	7.641	7.576
	5000	112.0	9.545	8.995	7.954	7.665	7.602
	5250	114.3	9.543	8.992	7.965	7.688	7.628
	5500	117.0	9.539	8.990	7.983	7.719	7.660

Straizys & Kuriliene (1981) for stars with spectral types F8 V and K1 V (in case a) or G0 V and K2 V (in case b) for the primary and secondary star, respectively.

On the other hand, we used the model atmospheres fluxes to compare synthetic and observed B, V, J, H, and K magnitudes out of eclipses, and to determine the distance to RT And. Even though the V magnitude of RT And at maxima was not measured at the same time as our IR photometry, and it also may show some variability the value $V=8.99$ that we deduce from the differential photometry of Dapergolas *et al.* (1991) is close to the value $V=9.01$ reported by Dean (1974). We used this value to derive the distance to RT And by comparison with the prediction of model atmospheres for the V magnitude. In any case, to use the observed V or K magnitudes at maxima to determine the distance, gives a difference of only 2 pc, smaller than the uncertainty that may be associated to the method used to derive it. The expected flux at Earth at any wavelength is calculated by means of the following expression:

$$f_{\lambda_i}=\frac{1}{D^2}\sum_{j=1}^{2} R_j^2 \pi F_{\lambda_i}^j, \tag{4}$$

where D is the distance to the system, R_j is the radii of the stellar jth component, and πF_λ is the surface flux from ATLAS atmosphere models. Solar abundances and $\log(g)$ $=4.0$ were always assumed in the models, being the model fluxes only weakly dependent on the $\log(g)$ value.

The expected magnitudes were calculated by convolving the flux distributions with the filters, the atmosphere and the detector's spectral response, with the absolute calibration adopted from Alonso *et al.* (1994). The values of the physical radii were derived from the relative radii of the IR light curves solutions, for both a and b cases and Popper's (1994) orbital solution (see the next section). The results are listed in Table 8 for a few combinations which produce colours not too far from the observed ones. Less importance should be given to the B synthetic magnitudes, as the photometry of RT

And indicates a B excess, and also because there are indications that the new ATLAS models underestimate the U,B fluxes. The comparison between the synthetic and observed magnitudes shows that the best agreement is given by radii in solution b, for primary star with an effective temperature $T_{\rm eff}\simeq 6000$ K and a secondary star with $T_{\rm eff}\simeq 5000$ K, located at a distance of 103 pc. In that case the differences between the synthetic and observed magnitudes out of eclipses are within 0.03 mag in the four filters V, J, H, and K. We have not intended to interpolate the best combination in the grid of model atmospheres, which have been used in $T_{\rm eff}$ steps of 250 K. We estimate the uncertainty in the $T_{\rm eff}$ determination using the grid of models in ± 125 K, but the real error could be larger if we considered the errors associated to the model's uncertainties. If we assume that the used radii values of the stars are reliable within 5%, similar precision in the fluxes predicted by the atmosphere models and absolute calibration of the photometry, an error in the observed magnitude out of eclipse of about 0.02 mag, and less than 150 K in the $T_{\rm eff}$ undetermination we can estimate that the distance determination is accurate within 10%. Other determinations of the distance to RT And have placed the star between 85 and 125 pc (Montle 1973; Dworak 1975).

3.4 The Absolute Dimensions of RT And

In the previous sections, we discussed the analysis of our infrared light curves of RT And, and showed that the solution arising from the IR light curves is in good agreement with other solutions previously derived by other authors from visual light curves (see Table 3), adding confidence to the derived absolute parameters of RT And's components. That point gains added importance due to the new radial velocity curves obtained recently by Wang & Lu (1993) and Popper (1994). The high dispersion spectroscopy, analyzed using modern procedures, provides new values for the spectroscopic parameters. Although in the next section we argue that our solution b seems to be the correct one, we have calculated the absolute masses and radii in both cases (a and b) in order to discuss the implications of the two solutions from the evolutionary point of view. Using Popper's radial velocity curve amplitudes, with the inclination angles and relative radii from our a and b solutions, we derived the absolute masses and radii of the stellar components of RT And:

Case a: $M_1=1.276\ \mathscr{M}_\odot,\quad R_1=1.206\ R_\odot,$

$M_2=0.933\ \mathscr{M}_\odot,\quad R_2=1.070\ R_\odot.$

Case b: $M_1=1.242\ \mathscr{M}_\odot,\quad R_1=1.270\ R_\odot,$

$M_2=0.906\ \mathscr{M}_\odot,\quad R_2=0.916\ R_\odot.$

Wang & Lu's (1993) orbital solution, yields values for the masses and radii of the stars which seem too small for their spectral types. We adopted Popper's (1994) solution, based on higher resolution observations than Wang & Lu's (1993) work, as the most reliable values at present. The new values for RT And's absolute masses and radii differ considerably from those currently accepted (Strassmeier *et al.* 1988). The mass ratio $q=0.73$ also indicates that RT And is a detached binary system. In the last section we will discuss the implications of these values in the masses and radii, comparing them with recently calculated evolutionary models for non-interacting stars.

Adopting values $T_{\rm eff\odot}=5780$ K and $BC_\odot=+4.69$ (Popper 1980) for the Sun, and applying the relation $M_{\rm bol}=42.31-5\log(R/R_\odot)-10\log(T_{\rm eff})$, we derive for the components of RT And: $M_{\rm bol}^{(1)}=4.0\pm0.20$ and $M_{\rm bol}^{(2)}=5.6\pm0.20$, for the primary and secondary component, respectively. Alternatively, using the visible magnitude out of eclipses $V=8.99$, the partial contribution of the primary star to the visible total light $L_V^{(1)}\simeq 0.86$, and the distance $d=103$ pc. to RT And, derived in the previous section, we derive the following values for the absolute magnitudes of RT And's components: $M_V^{(1)}=4.08\pm0.10$ and $M_V^{(2)}=6.0\pm0.25$.

4. WHICH OF THE TWO SOLUTIONS IS THE BEST

As can be seen in Tables 4 and 5, both a and b solutions give rather different values for the relative radius of the secondary component, as well as for the orbital inclination angle, and the relative luminosities L_1 and L_2 of the binary stellar components. Given the apparent undetermination in the light curve solutions, between the occultation or partial secondary eclipse cases, found in our analysis and in published results from visual light curves, we discuss this point further in order to clarify it and attempt to give a definitive solution. The previous analysis of the observed colours of RT And, after comparison with the colours of normal stars and model atmospheres predictions, is not conclusive and hence one of the two solutions cannot be discarded. However, three kinds of arguments can be used to distinguish between the two possibilities.

4.1 The Infrared Light Curve Fits

Even if our two solutions a and b give similar χ^2 fits, Figs. 5 to 8 show that solution b gives a better fit to the secondary eclipse depth in the both J and K light curves.

4.2 Eclipses Morphology

It is interesting to compare the visible light curves of RT And published to date. It is clear that this star has an intrinsic variability not only at levels of maxima, but also in the depth and symmetry of the secondary eclipse, which is probably the origin of the two classes of solutions found for the system (see Table 3). The first light curves from Gordon (1948, 1955) are well reproduced by an annular primary minimum and a total secondary minimum. Also, the secondary eclipse observed in 1962 by Dean (1974) in yellow light shows a flat bottom, suggesting an occultation. The same morphology of the secondary eclipse is shown by the 1990 and 1991 light curves of Dapergolas *et al.* (1991, 1992). Other published light curves usually show an asymmetric rounded secondary minimum, probably due to some photometric perturbation to the *normal* eclipse, producing a morphology that resembles a partial eclipse. We believe that the symmetric flat bottom secondary eclipse corresponds to the unperturbed state of the system, and so the occultation solution b gives the correct parameters for RT And's stellar components.

4.3 Spectroscopic Arguments

From a spectroscopic study of RT And, Popper (1994) estimates the contribution of the primary star to the total visible light to be $L_V^{(1)} \simeq 0.86$, which can be compared with the expected value in the cases of solutions a or b. From relation (2), the expected partial contribution of the primary star to the V filter light is

$$L_V^{(1)} = L_J^{(1)} 10^{0.4[(V-J)^{(b)} - (V-J)^{(1)}]}$$

or

$$L_V^{(1)} = L_K^{(1)} 10^{0.4[(V-K)^{(b)} - (V-K)^{(1)}]}, \tag{5}$$

where $L_J^{(1)}$ and $L_K^{(1)}$ are the partial contributions of the primary star to the total brightness in the filters J and K, respectively, $(V-J)^{(1)}$ and $(V-K)^{(1)}$ the colors of the primary component, and $(V-J)^{(b)}$ and $(V-K)^{(b)}$ the measured colours of RT And at maxima (Table 6). For the primary component we adopted the Johnson's (1966) expected colors for the spectroscopic F8 V type of the star. The partial contributions $L_J^{(1)}$ and $L_K^{(1)}$ are from our IR light curve solutions a and b (Tables 4 and 5).

For solution a, we have $L_V^{(1)}=0.76$, 0.77, while for solution b $L_V^{(1)}=0.89$, 0.93 (the two values for J and K data, respectively). If the primary star has a spectral type closer to G0 V than to F8 V, according to past classifications indicating its photometric colors, solution a: would turn out as $L_V^{(1)}=0.71$, 0.72, and solution b: as $L_V^{(1)}=0.84$, 0.87 (the two values for J and K data, respectively).

It seems clear that the spectroscopic estimate of the primary star contribution to the visual light is closer to what is expected from our solution b to the infrared light curves. Also, it is interesting that our estimate of $L_V^{(1)}$, from the infrared light curves solutions, is quite close to the value found in previous analyses of visual light curves which rendered similar solutions (see Table 3). The fact that similar values have been obtained from light curves observed at different wavelengths increases the confidence in the results.

Other arguments favouring solution b are presented in the next sections based on the comparison between the derived absolute masses and radii of RT And's components and evolutionary models predictions.

5. THE EVOLUTIONARY STELLAR MODEL AND COMPARISON WITH OBSERVATIONAL DATA

Evolutionary models were computed for the exact masses of RT And, considering the two possible solutions of the light curves for the orbital inclination and relative radii. This was done in order to avoid errors of interpolation on precomputed tables (recall that the mass of the primary is near the critical mass for which the predominant source of nuclear energy changes from pp reactions to the CNO cycle).

The computer code is basically the same as that described in our recent works (Claret & Giménez 1992; Claret 1995). The four differential equations are solved by means of the Henyey method for 400–700 mesh points and, as a boundary

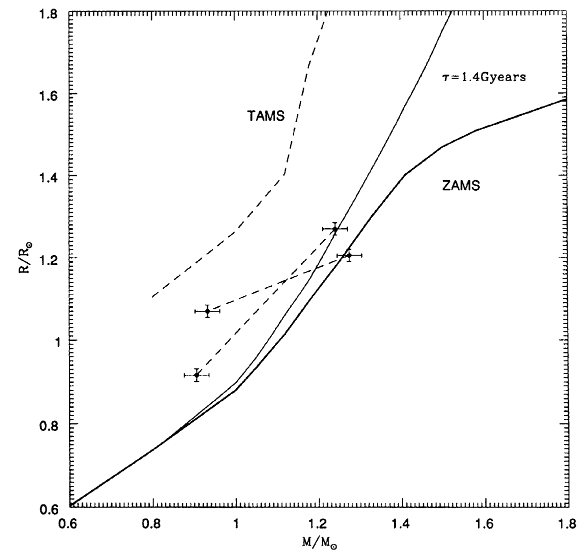

FIG. 9. $(\mathscr{M}/\mathscr{M}_\odot)-(R/R_\odot)$ diagram with a theoretical isochrone for the age 1.4×10^9 yr, and the ZAMS and TAMS lines. The primary and secondary components masses and radii are represented with the values from solution a and solution b.

condition in the outer layers, a gray atmosphere model is used. Integration in τ was carried out from 2 up to 1×10^{-4}. Core overshooting was considered for the components with masses around 1.2 $\mathscr{M}_\odot$. The parameter for the mixing length theory is 1.52, and for the core overshooting we adopted $\alpha_{ov}=0.20$, which seems to be representative of well binary stars with a good determination of absolute dimensions (see Claret & Giménez 1992, 1993a, 1993b). We adopted chemical composition values of: $(X,Z)=(0.70, 0.02)$.

The recent set of opacities (OPAL) provided by Iglesias *et al.* (1992), with spin-orbit coupling, were also adopted. These tables cover a larger range in temperatures and mainly in $R(\rho/T_6^3)$. For stellar envelopes where the temperatures are around and below 6000 K (which is the minimum temperature in OPAL tables) we used Alexander's (1992) results. Los Alamos (Huebner *et al.* 1977) tables were used in the range not covered by OPAL calculations.

The nuclear network treats 14 isotopes: H, ^{2}H, ^{3}He, ^{4}He, ^{12}C, ^{13}C, ^{14}N, ^{15}N, ^{16}O, ^{17}O (or ^{18}O), ^{20}Ne, ^{24}Mg, ^{28}Si, ^{56}Ni. The hydrogen network treats the three pp chains and the CNO cycle. The β decays, the abundance of ^{2}H and (^{7}Li+^{7}Be) are assumed to be in equilibrium. The screening factors were taken from Graboske *et al.* (1973), and the neutrino loss rates are from Munakata *et al.* (1985). The nuclear rates were taken from Fowler *et al.* (1975), Harris *et al.* (1983), Caughlan *et al.* (1985), and Caughlan & Fowler (1988). For the helium burning, and more details on the nuclear network, see Claret (1995).

In Fig. 9 we represent in a $(\mathscr{M}/\mathscr{M}_\odot)-(R/R_\odot)$ diagram the primary and secondary stars of RT And, with the absolute masses and radii derived following the two alternative solutions a and b, a theoretical isochrone for the age 1.4×10^9 yr and the theoretical ZAMS and TAMS lines. In the comparison between the derived absolute parameters of RT And's components and the theoretical evolutionary model predictions, the most reliable diagram must be the $(\mathscr{M}/\mathscr{M}_{\odot})-(R/R_{\odot})$, as the effective temperature $T_{\rm eff}$ is the most uncertain parameter of these stars. From that comparison we may conclude that solution b for radii and masses gives the best agreement with the theoretical models. In this case the primary component is located close to the isochrone of 1.4×10^9 yr, while the secondary star appears to be oversized for its mass.

Masses and radii in solution b lead to locating the primary star very close to the ZAMS, while the disagreement with theoretical expectations is worse for the secondary star. Given the reliability of the evolutionary models and of the physical parameters applied in the comparison, we may conclude that RT And is an abnormal binary system, in the sense that its stellar components do not seem to have evolved as isolated stars, even if at present it looks as a clearly detached system without evidence of significant interaction between the two stars. We have studied the effects of nonsolar composition on the theoretical isochrones, but the disagreement between the derived size of the secondary star with the theoretical expectation for its mass cannot be eluded by assuming an abnormal chemical composition in RT And.

6. CONCLUSIONS

We have obtained and reported here the first infrared light curves of RT And. We find some variability in the brightness of the system in this spectral range from one year to another. Part of the variations could be interpreted as due to the existence of cool starspots, but some transitory narrow features observed in the light curves must be related with absorptions by extra-photospheric matter.

Two different values for the relative radii of the stellar components and the orbital inclination are found in the light curve solutions, both in good agreement with other published solutions for visible light curves; a final optimal solution depends on the adopted set of initial parameters. However, we have shown that the intercomparison of previously published visual light curves, together with the information from spectroscopic studies and from our infrared photometry, indicates that the high inclination solution b (an occultation in the secondary eclipse) must be adopted as the correct one.

The observed colors of RT And are identical to those expected from the combination of two stars with spectral types G0 V and about K2 V, similar to those determined in spectroscopic studies. From the determination of the $(V-K)$ color for each stellar component of RT And, from the depth of the eclipses and the color out of eclipse, together with a modern calibration of $(V-K)$ vs $T_{\rm eff}$, we get for the effective temperatures of the stars: $T_{\rm eff}^{(1)}\simeq5950\pm70$ K and $T_{\rm eff}^{(2)}\simeq4880\pm100$ K for the primary and secondary star, respectively. Comparison between visual and infrared photometric magnitudes of the system out of eclipses and model atmosphere predictions, leads us to conclude that its fluxes are well reproduced by models with effective temperatures $T_{\rm eff}^{(1)}\simeq6000\pm150$ K and $T_{\rm eff}^{(2)}\simeq5000\pm100$ K for the primary and secondary star, respectively, at a distance of about 103 pc, and the absolute radii derived from solution b for our infrared light curves. Also we may discard any significant IR excess in the observed distribution. The derived effective temperatures of RT And components, $T_{\rm eff}^{(1)}\simeq6000$ K and $T_{\rm eff}^{(2)}\simeq4900$ K, are in good agreement with the $T_{\rm eff}$ spectral type calibration of Johnson (1966) for a F8 V ($T_{\rm eff}=6000$ K) or G0 V ($T_{\rm eff}=5900$ K) primary and a K2 V ($T_{\rm eff}=4960$ K) secondary. More recent calibrations of $T_{\rm eff}$ versus spectral type such as Straizys & Kuriliene's (1981), give $T_{\rm eff}=6150$ K for a F8 V, $T_{\rm eff}=5950$ K for a G0 V, and $T_{\rm eff}=4850$ K for a K2 V star. Then agreement between the derived $T_{\rm eff}$ and the spectroscopic classification is good for both stars, pointing to a spectral type of the primary closer to G0 V than to F8 V, as also indicated by its colours, while the $T_{\rm eff}$ of the secondary component is typical of a K2 V star.

Comparison of the derived absolute parameters for RT And components with the predictions made by evolutionary stellar models, also suggests that solution b is the right one. We find that whereas the primary star looks like as a normal star, close to the main sequence in the mass–radius diagram (Fig. 9), the secondary star seems to be oversized for its mass, and is located out of the main-sequence locus, with the particularly large disagreement for solution a values. If we accept the isochrone fitting to the primary star parameters from solution b, the age of the system can be estimated to be about 1.4×10^9 yr.

The impossibility to locate the primary and secondary star on an unique isochrone leads us to conclude that the evolution of the stellar components of RT And has not been normal; that is, their evolution has not been as isolated stars, and an episode of mass transfer between the stellar components during the main-sequence or pre-main-sequence evolution may be invoked, even if the system is now clearly detached.

The 1.5 Carlos Sánchez telescope is operated on the island of Tenerife by the Instituto de Astrofísica de Canarias at its Observatorio del Teide. The authors are grateful to Professors M. Zeilik and E. Budding for making available the programmes to fit the light curves, and to Professor P. Heckert for providing BD+52°3384 standard magnitudes. We also thank Monica Murphy for correcting the manuscript.

REFERENCES

Alexander, D. R. 1992, private communication
Alonso A., Arribas S., & Martinez-Roger C. 1994, A&A, 282, 684
Alonso A., Arribas S., & Martinez-Roger C. 1995, A&A (in press)
Al-Naimiy, H. M. 1978, ApJS, 53, 181
Arévalo, M. J., & Lázaro, C. 1990, AJ, 99, 983
Arévalo, M. J., & Lázaro, C. 1994, ASP Conf. Ser., 64, 545
Arévalo, M. J., & Lázaro, C. 1995, in preparation
Arribas, S., & Martinez-Roger, C. 1987, A&AS, 70, 303

Botsula, R. A. 1985, Izv. Astron. Ehngel'gardt Obs, 49, 62
Budding, E., Kadouri, T. H, & Giménez, A. 1982, Ap&SS, 88, 453
Budding, E., & Zeilik, M. 1987, ApJ, 319, 827
Caughlan, G. R., Fowler, W. A., Harris, M. J., & Zimmermann, B. A. 1985, Atomic Data Nucl. Data Tables, 32, 197
Caughlan, G. R., & Fowler, W. A. 1988, Atomic Data Nucl. Data Tables, 40, 283
Claret, A. 1995, A&AS, 109, 441
Claret, A., & Giménez, A. 1992, A&AS, 96, 255
Claret, A., & Giménez, A. 1993a, A&A, 277, 487
Claret, A., & Giménez, A. 1993b, in Inside the Stars, IAU Symposium No. 137, edited by W. W. Weiss and A. Baglin, PASPC, 469
Dapergolas A, Kontizas., E., & Kontizas, M. 1988, IBVS, No. 3267
Dapergolas A, Kontizas., E., & Kontizas, M. 1991, IBVS, No. 3661
Dapergolas A, Kontizas., E., & Kontizas, M. 1992, IBVS, No. 3818
Dapergolas A, Kontizas., E., & Kontizas, M. 1994, IBVS, No. 4036
Dean, C. A. 1974, PASP, 86, 912
Deichmueller, F. 1901, ANac, 157, 31
Drake, S. A., Simon, T., & Linsky, J. L. 1986, AJ, 91, 1229
Dumitrescu, A. 1973, Studii si Cercetari de Astron., 18, 47
Dumitrescu, A. 1974, Studii si Cercetari de Astron., 19, 89
Dworak, T. Z. 1975, AcA, 25, 383
Eaton J. A., & Poe, C. H. 1984, AcA, 34, 478
Fowler, W. A., Caughlan, G. R., & Zimmermann, B. A. 1975, AR&A, 13, 69
Gadomski, J. 1928, AcA, Ser. C., 1, 21
Gordon, K. J. 1948, AJ, 53, 198
Gordon, K. J. 1955, AJ, 60, 422
Gordon, S., Hall, S., Ledlow, M., Mann, E., & Zeilik, M. 1990, Inf. Bull. Var. Stars, No. 3469
Graboske, H. C, de Witt, H. E., Grossman, S. S., & Cooper, M. S. 1973, A&J, 181, 457
Hall, D. S. 1976, in Multiple Periodic Variable Stars, edited by W. S. Fitch (Reidel, Dordrecht), p. 287.
Harris, M. J., Fowler, W. A., Caughlan, G. R., & Zimmermann, B. A. 1983, AR&A, 21, 165
Heckert, P. 1994, private communication
Huebner, W. F., Merts, A. L., Magge, N. H., & Argo, M. F. 1977, Los Alamos Scientific Laboratory Report, LA-6760-M
Iglesias, C. A., Rogers, F. J., & Wilson, B. G. 1992, ApJ, 397, 771
Johnson, H. L. 1966, ARA&A, 4, 193
Koornneef, J. 1983, A&A, 128, 84
Kristerson, H. 1967, Bull. Astron. Inst. Czechoslovakia, 18 (5), 261
Kron, G. E. 1950, PASP, 62, 141
Kurucz, R. L. 1991, in Precision Photometry: Astrophysics of the Galaxy, edited by A. G. Davis Philip, A. R. Upgren, and K. A. Janes (Davis)
Lázaro, C., & Arévalo, M. J. 1994, ASP Conf. Ser., 64, 435
Lynds, B. 1962, ApJS, 7, 1
Mancuso, S., Milano, L., & Russo, G. 1979a, A&AS, 36, 415
Mancuso, S., Milano, L., Russo, G., & Sollazzo, C. 1979b, A&AS, 38, 187
Mancuso, S., Milano, L., Russo, G., & Sollazzo, C. 1979c, Ap&SS, 66, 475
Mancuso, S., Milano, L., Vittore, A., Budding, E., & Jassur, D. M. Z. 1981, in Photometric and Spectroscopic Binary Systems, edited by E. B. Carling and Z. Kopal (Reidel, Dordrecht), p. 313
Milano, L. 1981, in Photometric and Spectroscopic Binary Systems, edited by E. B. Carling and Z. Kopal (Reidel, Dordrecht), p. 331
Milano, L., Russo, G., & Mancuso, S. 1981, A&A, 103, 57
Milano, L., Mancuso, S., Vittore, A., D'Orsi, A., & Marcozzi, S. 1986, Ap&SS, 124, 83
Montle, R. E. 1973, Master thesis, Vanderbilt University, Nashville, TN, p. 36
Munakata, H., Kohyama, Y., & Itoh, N. 1985, ApJ, 296, 197
Payne-Gaposchkin, C. 1946, ApJ, 103, 191
Piotrowski, S. L., Rucinski, S. M., & Semeniuk, I. 1974 AcA, 24, 389
Popper, D. M. 1980, ARA&A, 18, 115
Popper, D. M. 1993, ApJ, 404, L67
Popper, D. M. 1994, AJ, 108, 1091
Straizys, V., & Kuriliene, G. 1981, Ap&SS, 80, 353
Strassmeier, K. G., Hall, D. S., Zeilik, M., Nelson, E., Eker, Z., & Fekel, F. 1988, ApJS, 72, 291
Wang, X. M., & Lu, W. 1993, in New Frontiers in Binary Star Research, ASP Conf. Ser. 38, 280
Wilson, R. E., & Devinney, E. J. 1971, ApJ, 166, 605
Wood, D. B. 1971, AJ, 76, 701
Wood, D. B. 1972, A computer code for modelling non-spherical eclipsing binary systems, GSFC
Zeilik, M., Elston, R., Henson, G., Scholke, P., & Smith, P. 1982, Inf. Bull. Var. Stars, No. 2090
Zeilik, M., Beckert, D., de Blasi C., Ledlow, M., Rhodes, M., & Williams, T. 1988a, Inf. Bull. Var. Stars, No. 3173
Zeilik, M., de Blasi, C., Rhodes, M., & Budding, E. 1988b, ApJ, 332, 293
Zeilik, M., Beckert, D., Cox, D. A., Dolby, J., Ledlow, M., & Newberry, M. 1989a, Inf. Bull. Var. Stars, No. 3301
Zeilik, M., Cox, D. A., de Blasi, C., Rhodes, M., & Budding, E. 1989b, ApJ, 345, 991
Zinner, E. 1916, Astron. Abh., 4, C5